

## UV Oxidation: Mechanistic Insights Using a Model System

JENNIFER M. MARSH, STEPHANIE L. DAVIS, RUI FANG, MONIQUE S. J. SIMMONDS,  
PHILIP GROVES AND VICTOR CHECHIK

*The Procter & Gamble Company, Mason Business Center, Mason, Ohio, USA*  
(J.M.M., S.L.D.)

*Royal Botanic Gardens, Kew, Richmond, Surrey, United Kingdom (R.F., M.S.J.S.)*

*Department of Chemistry, University of York, Heslington, York, United Kingdom (P.G., V.C.)*

### Synopsis

Damage to hair by UV radiation is relevant to most people, and for many, it is a major source of hair damage. The chemistry is complex, and studying all of the detailed reactions is extremely challenging. The objective of this work was to create a model system that allows for the study of one key mechanism involved in UV damage: the oxidation of tyrosine. A colloidal system to study the reactivity and chemistry of tyrosine was tracked by monitoring tyrosine decomposition and dityrosine formation by fluorescence spectroscopy. Experiments showed both the important role of oxygen in the decomposition of tyrosine and how the addition of redox metals such as iron can accelerate this decomposition. Finally, an antioxidant, butylated hydroxytoluene, was demonstrated to reduce this oxidation through the interception of reactive oxygen species. These findings suggested two possible strategies for reducing UV-induced radical damage to hair: removal of redox metals and addition of a radical scavenger to react with reactive oxygen species formed. The second strategy was confirmed by testing selected extracts from tea (*Camellia sinensis*), which is well known to have antioxidant properties. An oxygen radical antioxidant capacity assay was used as a screening tool to identify which tea extracts have the highest antioxidant efficacy, and these extracts were shown to reduce UV-induced protein damage in hair.

### INTRODUCTION

Healthy hair is described as hair that has shine, can be readily styled, and has low levels of frizz in high humidity. In contrast, damaged hair shows signs of breakage, lack of alignment, split ends, and frizz (1). This difference is driven by multiple insults including oxidative colorants, UV exposure, heat, and physical damage from grooming habits such as washing and combing. Exposure to too much sun leading to lighter hair and damaged tips is a well-recognized issue for women, and breakage is often observed after prolonged exposure. Degradation of different parts of the hair structure by UV radiation has been well-documented in the literature, with changes to cuticle and cortex protein structures (2), cell membrane lipids (3), and melanin (4).

---

Address all correspondence to Jennifer M. Marsh, marsh.jm@pg.com

The different chemical mechanisms causing these changes are complex and difficult to measure directly in hair. There is strong evidence that two key amino acids in hair that absorb UV-B radiation are tryptophan and tyrosine. These amino acids are photoionized and produce aromatic free radicals. Tryptophan oxidation produces yellow-colored kynurenines (5), which can be observed as a photo-yellowing effect in light-colored hair. Singlet oxygen and a superoxide radical anion are formed by the photosensitization of both aromatic amino acid residues and melanin pigments (6). Cell membrane complex unsaturated lipids such as the unsaturated fatty acids react with singlet oxygen to form hydroperoxides that modify the cell membrane complex and provide hydroxyl and alkoxy radicals for additional reactions. These reactions have been studied and reported in both hair and wool (2,7). Reactive oxygen species (ROSs) that are formed continue to propagate damage throughout the hair. It has also been shown that redox metals such as copper can accelerate these radical reactions and create additional protein damage (8).

An approach to reducing UV damage is to terminate the reactions by quenching free radicals or ROSs. Primary antioxidants, such as polyphenols, act in this manner. There are three main mechanisms by which antioxidants can scavenge ROSs: hydrogen-atom transfer, single-electron transfer, and metal chelation. Polyphenols can act as antioxidants by these mechanisms and are important because they are commonly found in botanical extracts including tea (*Camellia sinensis*) (9). Several publications have studied the use of tea extract for hair and skin benefits (10), including as protection against UV-induced skin damage and in the development of sunscreen products (11). Tea extracts have also been studied for their impact on hair growth (12) and sebum reduction (13).

The objective of this study was to create a model system for the key components in hair involved in the initiation of radical pathways and gain a more detailed understanding of specific pathways involved, including the role of redox metals. From this work, the strategy of adding antioxidants was identified as an option for reducing oxidative damage. A selection of tea extracts that can prevent UV damage by intercepting the ROSs formed were screened and shown to reduce this oxidative damage.

## MATERIAL AND METHODS

### POLY(ETHYLENE GLYCOL)–TYROSINE BLOCK COPOLYMER MICELLES

Poly(ethylene glycol)–tyrosine (PEG–Tyr) polymers (prepared according to published literature procedures [14]) were kindly donated by Prof. A. Heise, Dublin City University, Dublin, Ireland (14). PEG<sub>5000</sub>–Tyr<sub>15</sub> (20 mg, 0.00259 mmol), PEG<sub>2000</sub>–Tyr<sub>5</sub> (10 mg, 0.00344 mmol), and PEG<sub>5000</sub>–Tyr<sub>10</sub> (20 mg, 0.00293 mmol) were separately added to water (1 mL). The mixtures were sonicated at room temperature for 60 min to ensure homogenous dissolution into colloidal systems.

The colloidal systems were irradiated using a 100 W mercury arc lamp (Oriel 6281/Ushio USH-102DH) with spectral irradiance ranging from deep UV through infrared wavelengths.

To add iron(III) stearate and iron(III) acetylacetonate to the polymer, stock Fe(III) solutions were prepared. Specific volumes of the stock solution were transferred into sample vials to give the desired metal concentration when diluted by a factor of 100. The ethanol was then removed under a vacuum, and PEG<sub>2000</sub>–Tyr<sub>5</sub> polymer solutions (0.5–5 mg/mL, 0.074–0.735 mM) were prepared in 0.1 M pH 5 acetate buffer and added to dried Fe residue. The

resulting solutions were shaken for 1 h, sonicated for 1 h, and then shaken for an additional 1 h to ensure partitioning of the hydrophobic metal salt into the colloidal system.

#### FLUORESCENCE ANALYSIS OF COLLOIDAL SYSTEMS

After each sample had been irradiated, 150  $\mu\text{L}$  of ethanol was added to dissolve any aggregates. Then, 200  $\mu\text{L}$  of the resulting solution was withdrawn, and 400  $\mu\text{L}$  of each 0.1 M pH 5 acetate buffer and 0.4 M pH 8.5 borate buffer was added. This decreased the ethanol concentration sufficiently for micelle structures to form, as tested by dynamic light scattering. Fluorescence excitation and emission spectra were recorded, with an average of three scans taken for each sample. (Excitation parameters: emission wavelength, 303 nm; excitation scan, 240–300 nm. Emission parameters: excitation wavelength, 276 nm; emission scan, 270–500 nm.) Dityrosine fluorescence was also monitored. (Excitation parameters: emission wavelength, 405 nm; excitation scan, 240–400 nm. Emission parameters: excitation wavelength, 320 nm; emission scan, 325–550 nm.) The extent of tyrosine degradation was measured as a percentage decrease in the tyrosine emission maximum intensity at 310 nm relative to the dark control for each sample. Fluorescence measurements were performed on a Hitachi F-4500 fluorescence spectrophotometer using  $1 \times 1$  cm quartz cells.

Samples were treated after irradiation to remove metals before fluorescence measurements were made. Iron was removed from the samples by the precipitation as  $\text{Fe}(\text{OH})_3$  at high pH: To 140  $\mu\text{L}$  samples was added 150  $\mu\text{L}$  of dilute NaOH solution (194 mM). Samples were shaken and left for 10 min for precipitation to occur and were then filtered through 450 nm polytetrafluoroethylene filters.

#### BUTYLATED HYDROXYTOLUENE (BHT) EXPERIMENTS

For studies with butylated hydroxytoluene (BHT) antioxidant, a stock BHT solution in ethanol at a concentration of 1.5 mM was prepared. Specific volumes of the stock solution were transferred into sample vials to give the desired BHT concentration when diluted by a factor of 100. The ethanol was then removed under a vacuum, and PEG<sub>2000</sub>-Tyr<sub>5</sub> polymer solutions (0.5–5 mg/mL, 0.074–0.735 mM) were prepared in 0.1 M pH 5 acetate buffer and added to dried BHT residue. The resulting solutions were shaken for 1 h, sonicated for 1 h, and then shaken for an additional 1 h to ensure partitioning of the hydrophobic antioxidant into the colloidal system.

#### HAIR

Human hair for the testing was purchased from International Hair Importers & Products, Glendale, New York. Natural white hair, a hair type that is very low in melanin content, was used for UV biomarker work.

#### HAIR TREATMENTS

For biomarker experiments, natural white hair was treated with solutions containing 5% *C. sinensis* extract. These solutions were applied to wet hair and left to dry without rinsing. The resulting samples were compared to baseline untreated hair and UV-exposed-only

hair (no *C sinensis* treatment). Hair was exposed to artificial radiation using the settings described in the next section for a total of 60 h. After 20 and 40 h of irradiation, the hair was washed with a clarifying shampoo, and tea solutions were reapplied. The hair was washed again with clarifying shampoo before extraction.

#### EXPOSURE TO ARTIFICIAL RADIATION

Hair samples were exposed to simulated sun exposure with an Atlas Ci3000+ Weather-Ometer® (Atlas, Chicago, Illinois). Both internal and external quartz filters were used to simulate broad-spectrum, outdoor daylight with a specific irradiance of 1.48 W/m<sup>2</sup> at 420 nm. During the irradiation process, temperature and relative humidity (RH) were kept constant at 35°C and 80% RH, respectively. This amount of irradiation for a total of 60 h simulates and is approximately equivalent to 40 min/d of summer sunlight exposure for 3 months in Miami, Florida.

#### OXYGEN RADICAL ANTIOXIDANT CAPACITY (ORAC) MEASUREMENTS

An OxiSelect™ oxygen radical antioxidant capacity (ORAC) activity assay kit was purchased from Cell Biolabs (San Diego, California). For each measurement, a fluorescent probe solution was freshly prepared by diluting stock solution in the assay diluent. A water-soluble analogue of vitamin E, Trolox™ (6-hydroxy-2,5,7,8-tetramethylchroman-2-carboxylic acid) (Hoffman-LaRoche, Nutley, New Jersey), was used as the standard material. Antioxidant working standard solutions were freshly prepared by diluting 5 mM Trolox™ stock solution in assay diluent. Serial dilution of extract solutions was performed with assay diluent to ensure that the samples were within the calibration curve range and demonstrated dilution integrity. Aliquots (25 µL) of each antioxidant working standard or sample and 150 µL of fluorescent probe solution were added to the predesignated well in a 96-well clear-bottom black plate. The plate was then allowed to equilibrate by being incubated for 30 min at 37°C. Free-radical initiator solution was freshly prepared at 80 mg/mL in undiluted phosphate-buffered saline. Reactions were initiated by the addition of 25 µL of free-radical initiator solution into each well. Fluorescence signals were read with a Spectramax M3 multimode microplate reader using SoftmaxPro 7.0 software (Molecular Devices, San Jose, California) at 37°C with an excitation wavelength of 480 nm and an emission wavelength of 520 nm for 60 min in increments of 3 min. The final assay values of the blank control should be less than 10% of the initial values for the assay to be completed. A calibration curve was constructed by plotting the differences in the areas under the fluorescence kinetic decay curves against the Trolox™ antioxidant standard concentrations. The ORAC value of the extract solution was determined by back-calculation using a linear regression of the calibration curve and was expressed in terms of micromoles of Trolox™ equivalents after a correction for the dilution factor was applied.

#### BIOMARKER ANALYSIS

Samples (0.5 g) of hair from treated tresses were cut and placed into 50 mL tubes with 5 mL of water added. Tubes with hair and water were mixed on a multitube vortex shaker for 60 min at 2,500 rpm. The water portion was then transferred from the tubes by pipette

into glass scintillation vials. A 10 mg/mL solution of matrix-assisted laser desorption/ionization (MALDI) matrix ( $\alpha$ -cyano-4-hydroxycinnamic acid) was mixed with the hair extract samples in a 1:1 volume ratio. Then, 1  $\mu$ L of this solution was used to spot on the MALDI plate, and a MALDI mass spectrum was acquired (1,000 shots). The intensity of the UV damage marker peptide at  $m/z$  1,278 was measured. This biomarker was identified as a fragment of the S100A3 protein that is involved in cuticle cell adhesion (24) and is directly related to the level of UV exposure of untreated hair.

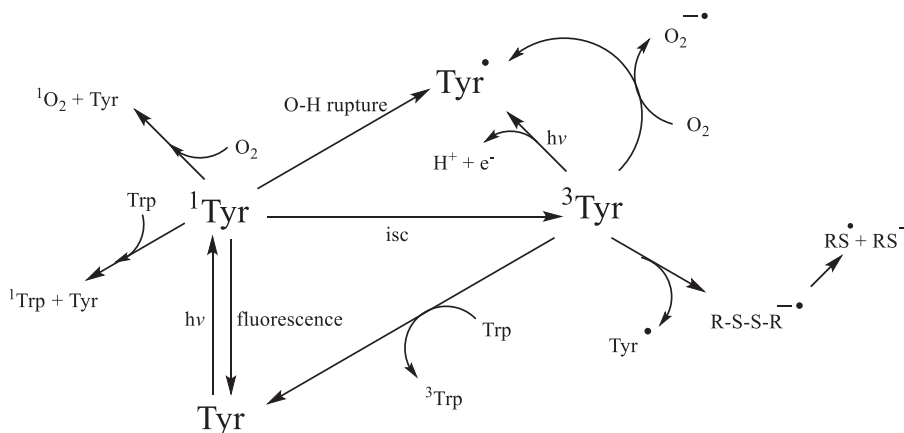
#### CAMELLIA SINENSIS (TEA) EXTRACTS

Commercially available *C sinensis* extracts and powders were obtained from seven suppliers of botanical ingredients. The materials were described by the suppliers as either green or white (nonfermented) tea extracts. The number of samples per supplier varied from one to three. Each material was assigned a unique five-digit botanical identification code (BIC). BICs are used to identify the materials throughout this article. Details about the chemistry of these extracts were published by Davis et al. (31). A summary of the findings are presented here to support the role of catechin compounds in reducing oxidative damage and the role of the ORAC assay in evaluating this activity.

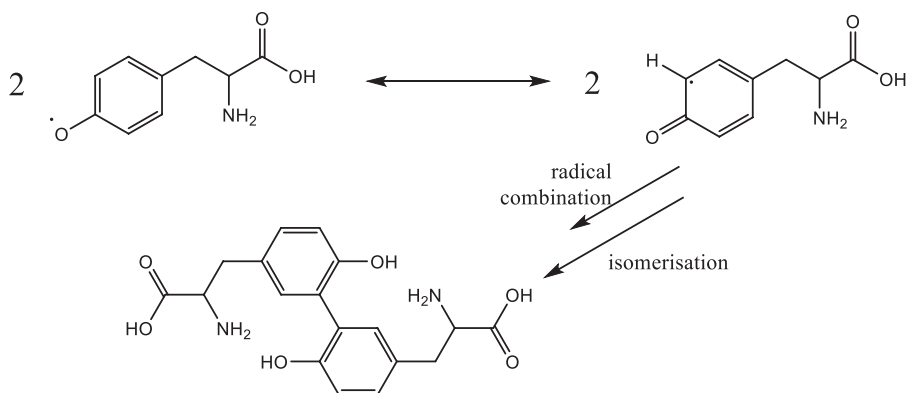
## RESULTS AND DISCUSSION

### PHOTOCHEMISTRY MODEL SYSTEM

The only amino acids capable of direct photoexcitation by sunlight are those with significant absorption above 280 nm. These are limited to those with aromatic side chains: tryptophan, tyrosine, phenylalanine, and histidine (although phenylalanine and histidine do not absorb significantly at 280 nm) (15). Tryptophan is the most effective UVB-absorbing chromophore among the aromatic amino acids, but given that tyrosine has far greater abundance than tryptophan in many keratin proteins (16) and hair overall (17), it is likely that tyrosine photochemistry is relevant to the overall photochemistry of hair proteins. In



Scheme 1. Summary of the main reaction pathways of tyrosine upon photoexcitation (20–22).



Scheme 2. Formation of dityrosine by the combination of two tyrosyl radicals.

aqueous solution at neutral pH, tyrosine exhibits two absorption bands at wavelengths of about 220 and 275 nm, which are assigned to  $\pi$ - $\pi^*$  transitions (18). Upon absorption of a photon, the amino acid is excited to the first singlet excited state. The subsequent pathways are shown in Scheme 1.

Once formed, tyrosyl radicals can undergo a wide variety of reactions. Two radicals can combine through either a C-C linkage or a C-O linkage to form dityrosine (19) (Scheme 2).

Initial experiments were performed on tyrosine itself, but its photochemistry was not amenable to study. In solution, any tyrosyl radicals formed were too short-lived to be studied, but as a solid, the radicals that formed persisted for many hours. These data highlighted the importance of the molecular environment for photochemistry pathways. This phenomenon has also been seen in hair studies in which protein degradation was found to be highly dependent on relative humidity (23).

The aim in this work was to create a system with a restricted tyrosine environment that still allowed for some molecular mobility. Toward this end, a series of amphiphilic PEG-Tyr block copolymers were used (Figure 1) (14). The hydrophilicity of the PEG block and the hydrophobicity of the Tyr block cause the copolymers to self-assemble into kinetically trapped, stable colloidal structures upon dissolution in water. Upon heating, the solutions spontaneously convert into more thermodynamically stable gels (24).

Fluorescence spectroscopy was used to monitor the loss of tyrosine and formation of dityrosine. Samples were irradiated in 1 cm-path-length quartz cuvettes. Initial experiments used the PEG<sub>5000</sub>-Tyr<sub>10</sub> polymer irradiated for 3 and 24 h, with fluorescence of the sample measured relative to that of a control sample prepared at the same time but kept in the

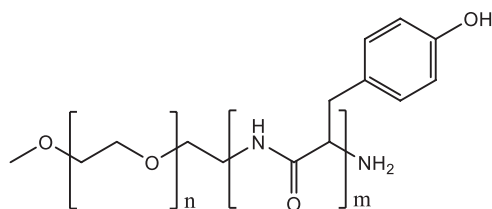
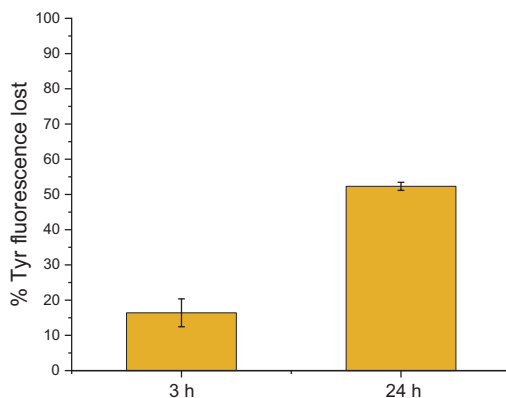


Figure 1. Structure of PEG-Tyr block copolymers.



**Figure 2.** Tyrosine degradation upon UV exposure of a 10 mg/mL PEG<sub>5000</sub>-Tyr<sub>10</sub> aqueous micellar solution, measured in terms of the decrease in tyrosine fluorescence relative to that of a control sample.

dark. The degradation measured after the 3 h exposure period was 16%. Over a 24 h exposure period, 52% degradation was observed (Figure 2).

Experiments were then performed with iron chloride salts to understand the role of redox metals in ROS formation. Increased tyrosine degradation was found, but iron levels greater than 100 ppm were needed because of the lower solubility of chloride salts in the PEG-Tyr micelles. Thus, two hydrophobic iron(III) salts that can localize into the polymer micelles were used, namely, iron(III) stearate [Fe(stearate)<sub>3</sub>] and iron(III) acetylacetonate [Fe(acac)<sub>3</sub>]. The percentage tyrosine degradation was measured over 24 h as a function of added Fe(stearate)<sub>3</sub>. Even at very low metal concentration (0.1 μg/g), the degradation was found to be significantly higher than in the metal-free systems (Figure 3). This iron salt

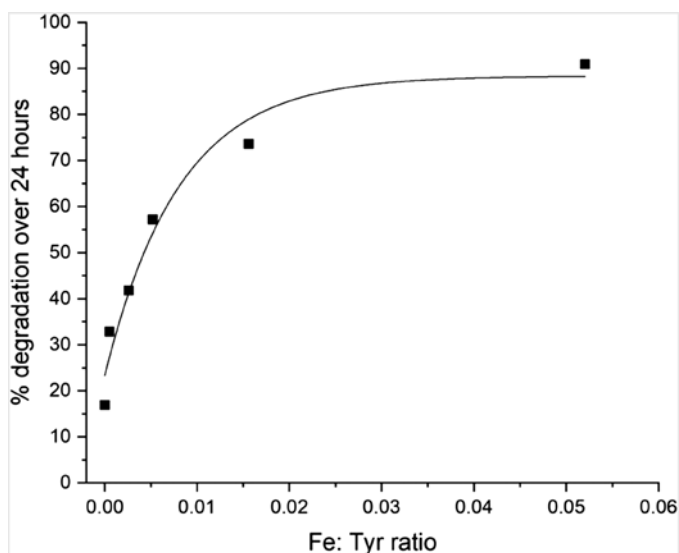


**Figure 3.** Effect of the Fe(stearate)<sub>3</sub> concentration (expressed as the Fe:Tyr ratio) on tyrosine degradation in PEG<sub>2000</sub>-Tyr<sub>5</sub> micellar systems at 2 mg/mL, measured in terms of the decrease in tyrosine fluorescence over 24 h of UV exposure.



Table I  
Percentage Loss of Photochemical Activity in Air-Free Samples, Compared to Identical Samples in Air\*

	PEG <sub>5000</sub> -Tyr <sub>10</sub> , no metal	PEG <sub>2000</sub> -Tyr <sub>5</sub> , 0.5 ppm Fe(stearate) <sub>3</sub>	PEG <sub>2000</sub> -Tyr <sub>5</sub> , 0.5 ppm Fe(acac) <sub>3</sub>
Tyr degradation	94	18	89
Dityrosine formation	87	93	95

\*Based on fluorescence data, rounded to the nearest whole number.

was found to have less of an impact on degradation at higher concentration because of its lack of solubility.

The role of oxygen was then investigated by comparing the rates of tyrosine degradation and dityrosine formation in both a metal-free polymer system (PEG<sub>5000</sub>-Tyr<sub>10</sub>) and a polymer system (PEG<sub>2000</sub>-Tyr<sub>5</sub>) containing 0.5 ppm Fe(III) as either stearate or acetylacetonate. The solutions were degassed and then sealed and irradiated for 24 h before being analyzed by fluorometry (Table I).

In terms of tyrosine oxidation, both metal-containing systems were less affected by the exclusion of oxygen than the metal-free system. This indicates that direct metal-tyrosine interactions play a role in Tyr degradation. Furthermore, the system containing Fe(stearate)<sub>3</sub> was much less influenced by the exclusion of oxygen. This is likely because, in this case, the iron was immobilized within the micelle and the direct interaction between iron and tyrosine was significantly enhanced, contributing to more overall degradation. Excluding oxygen therefore has less of an impact for Fe(stearate)<sub>3</sub> than for Fe(acac)<sub>3</sub>, for which increased activity primarily arises from increased ROS production.

Although dityrosine formation was found to occur in the absence of oxygen, in agreement with the literature (25), its formation was significantly suppressed under oxygen-free conditions. This is indicative of a lower radical yield, as excited-state tyrosine cannot transfer an electron to molecular oxygen. Despite increased dityrosine formation compared to the metal-free system, the iron(III) samples were affected in a similar way when air was removed. This suggests that metal complexes are not effective electron acceptors and increased activity through direct metal-tyrosine interaction could therefore arise from the photosensitization of tyrosine by metal complexes.

To determine whether antioxidants could reduce tyrosine degradation, BHT was identified as a suitable candidate because it is relatively hydrophobic and acts by donating the phenolic proton to quench peroxy radical species. This creates a phenoxyl radical that is stabilized through conjugation to the aromatic ring and steric hindrance provided by the *tert*-butyl groups in ortho positions (26).

BHT was found to have a significant impact on the observed photodegradation of tyrosine over a prolonged exposure period in a metal-free system and when iron(III) was present as stearate and acetylacetonate complexes (Table II). However, the different iron complexes exhibited notably different responses to the antioxidant. Both metal-free and Fe(acac)<sub>3</sub> systems show a rapid drop-off at low antioxidant concentration indicative of BHT effectively quenching peroxy radicals, thus breaking the autoxidation cycle. By comparison, addition of a low concentration of BHT to Fe(stearate)<sub>3</sub>-containing samples results only in a modest decrease in activity, as also seen in air-free experiments because of the direct interaction between the metal and tyrosine.

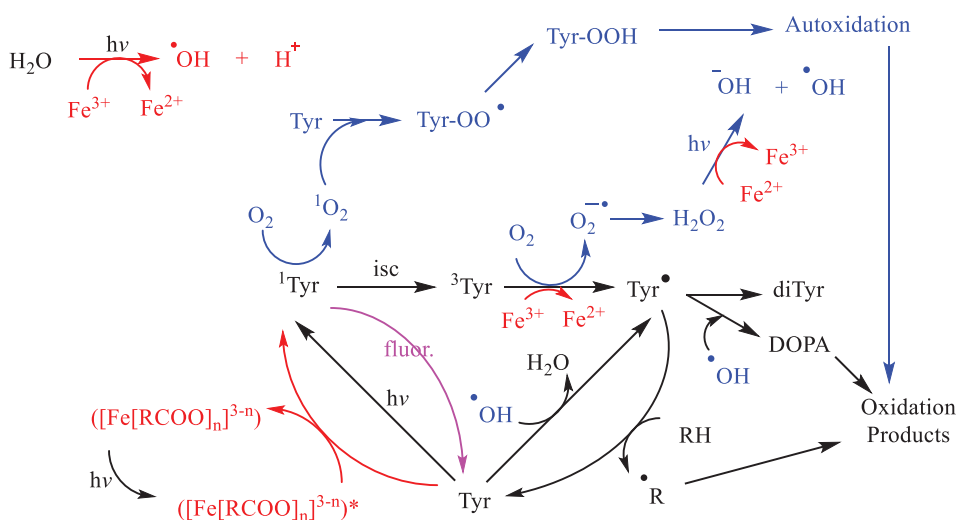


**Table II**  
Effect of BHT at Low Concentration on Tyrosine Degradation Over 24 h in 0.172 mM PEG<sub>2000</sub>-Tyr<sub>5</sub> Micellar Systems

System	Degradation (%)		
	No BHT	0.05 mM BHT	Suppression by antioxidant
No metal	16.7	5.9	64.7
0.5 ppm Fe(stearate) <sub>3</sub>	28.0	26.6	5.0
0.5 ppm Fe(acac) <sub>3</sub>	66.0	22.4	66.1

From these data, a reaction scheme can be proposed (Scheme 3) for possible pathways following the excitation of tyrosine by UV irradiation. Multiple pathways are involved, but it has been shown that redox metals, such as iron, and oxygen play an important role in degradation and antioxidants such as BHT can intercept at least some of these pathways.

This information identifies several strategies for potentially reducing UV-induced oxidative damage in hair. The first is the removal of redox metals to prevent the acceleration of radical formation, as shown in Scheme 3. This strategy has been demonstrated to be successful in the case of copper removal (27). The second is through the addition of antioxidants that can scavenge the ROSs formed. The literature on wool has indicated success with this strategy in protecting wool from photoyellowing (28). More recently, botanical extracts that have traditionally been used as antioxidants in food have also been shown to provide benefits to hair. Protein protection has been measured for artichoke (*Cynara cardunculus* var. *scolymus* L.) and rice grain (*Oryza sativa* L.) extracts (29). However, none of these studies included an analysis of extract compositions or a correlation between the antioxidant activity of these botanical extracts and the prevention of hair damage.



**Scheme 3.** Summary of tyrosine degradation in model systems. Oxygen-dependent pathways are shown in blue; the involvement of iron is shown in red.

## TEA EXTRACTS

In this work, tea (*C sinensis*) was the chosen botanical antioxidant to test its ability to scavenge reactive oxygen species in the presence of UV radiation. It is rich in polyphenols and has been shown to deliver benefits to both skin and hair (10). Several publications have studied the use of tea extracts as protection against UV-induced skin damage and in the development of sunscreen products (11,30). Tea extracts have also been studied for their impact on hair growth (12) and sebum reduction (13). In an earlier study, 16 tea extracts were chosen, and their antioxidant abilities were tested by ORAC assay (31). This assay is commonly used to measure the antioxidant capacities of foods such as teas, fruits, and vegetables, and it measures inhibition of peroxy-radical-induced oxidations by the hydrogen-atom-transfer mechanism, a mechanism relevant to human biology and hair. The azo initiator 2,2'-azobis(2-amidinopropane) dihydrochloride is used to generate peroxy radicals, and a fluorometer is used to measure the rate at which the formed radicals oxidatively degrade an added fluorescent molecule (fluorescein). Table III reports the ORAC data from the 16 tea samples tested and shows that the ORAC scores ranged over three orders of magnitude from 92 to 3,413,500  $\mu\text{M}$  Trolox™ equivalents (TE).

Liquid chromatography/mass spectrometry was used to measure the compositions of the 16 tea samples, and a total of 42 compounds were detected, of which 34 were identified; full details of the compounds identified are available in Davis et al. (31). The majority of extracts contained low levels of all compounds, with the exception of the four tea samples with BICs 29455, 29458, 29462, and 29465. These four extracts contained similar profiles

Table III  
ORAC Scores for *C sinensis* (Tea) Extracts\*

BIC	Tea type	Form	Delivery	ORAC score ( $\mu\text{M}$ TE/100 g)	Standard deviation
29465	Green	Powder	Made up to 5%	3,413,500	241,123
29458	Green	Powder	Made up to 5%	1,897,076	45,142
29455	Green	Powder	Made up to 5%	1,500,536	49,262
29462	Green	Powder	Made up to 5%	1,454,008	181,366
29459	Green	Liquid	10–25% in propylene glycol	108,702	40,091
29471	Green	Powder	5% with maltodextrin	71,797	10,341
29464	Green	Liquid	Unknown conc. in glycerin	46,920	2,969
29463	White	Liquid	10% in propylene glycol	42,635	7,840
29469	Green	Liquid	5% in glycerin	40,580	23,079
29457	Green	Liquid	5% in glycerin	22,861	6,554
29467	White	Liquid	Unknown conc. in propylene glycol	15,098	2,303
29470	White	Liquid	Unknown conc. in glycerin	7,980	654
29460	Green	Liquid	Unknown conc. in glycerin	3,028	62
29456	White	Liquid	Unknown conc. in glycerin	1,747	174
29466	White	Liquid	Unknown conc. in glycerin	1,025	186
29461	White	Liquid	Unknown conc. in glycerin	92	13

\*Reproduced with permission from Scientific Research Publishing, Inc. (31).

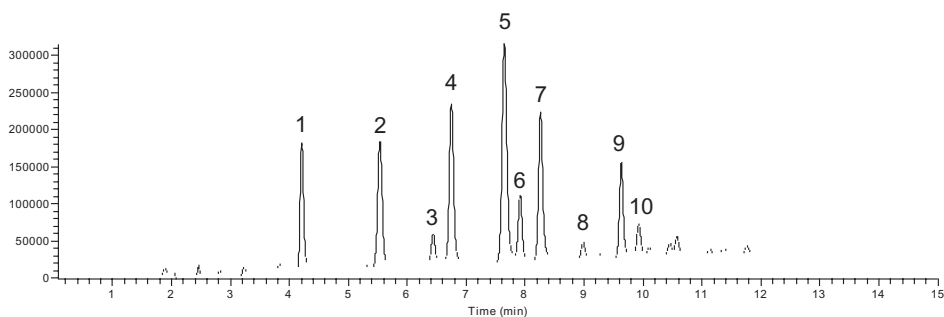


**Figure 4.** Chromatogram of tea sample BIC 29465. Major compounds: 1, gallic catechin; 2, (–)-epigallocatechin; 3, (+)-catechin; 4, caffeine (procyanidin B peak lies behind this peak); 5, epigallocatechin gallate; 6, (–)-epicatechin; 7, gallic catechin gallate; 8, (–)-epigallocatechin-3-(3′-O-methyl) gallate; 9, (–)-epicatechin gallate; 10, (–)-catechin gallate.

of catechin compounds and caffeine (Figure 4), whereas extracts with low ORAC scores contained lower levels of these compounds.

A correlation between the ORAC scores and the identified components showed that (–)-epicatechin and procyanidin B had the largest correlation coefficients, and most catechins in the tea samples significantly correlated ( $p < 0.001$ ) with the ORAC scores (31).

#### HAIR UV BIOMARKER EXPERIMENTS

Previously published work has shown that the exposure of hair to UV radiation produces protein damage (2) and that MALDI time-of-flight (TOF) mass spectrometry (MS) can be used to identify specific fragments that correlate with total protein damage and UV

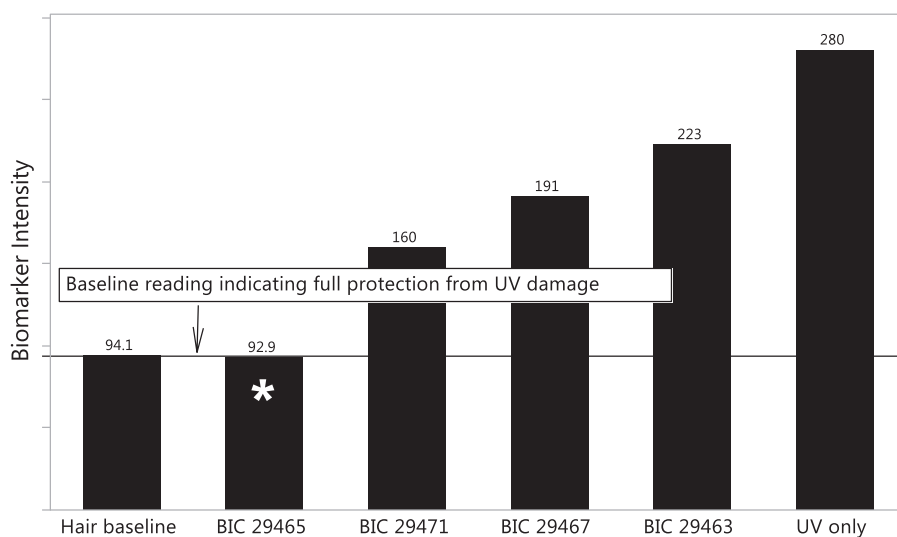


**Figure 4.** Protection from damage as measured by UV biomarker intensity ( $m/z$  1,278). \*,  $p < 0.05$  versus UV-only, Student's t-test. Reproduced with permission from Scientific Research Publishing, Inc. (31).

exposure (8). Specifically, a marker peptide at  $m/z$  1,278 was identified as a fragment of the S100A3 protein known to be involved in cuticle cell adhesion (32). Hair treated with four of high activity tea extracts was exposed to UV radiation and compared to hair with no treatment exposed to UV radiation and hair with no UV exposure. After UV exposure the protein biomarker at  $m/z$  1,278 was extracted in water and quantified by MALDI-TOF MS. A significant increase in biomarker peak intensity was measured for hair that had been pretreated with tea extracts, illustrating a protective benefit. The magnitude of this benefit was correlated to the concentration-adjusted ORAC score ( $R^2 = 0.98$ )

## CONCLUSION

The UV oxidation of proteins entails complex chemistry involving reactive oxygen species, and tracking this chemistry in hair is extremely challenging. Our approach has been to use a model colloidal system incorporating tyrosine, a key amino acid involved in UV-induced protein damage. Using this colloidal system, we identified the roles of oxygen, reactive oxygen species, and redox metals such as iron in the oxidation of tyrosine. Also demonstrated with this model system was the ability to decrease oxidation through the addition of antioxidants such as BHT. Experiments on hair were performed with selected botanical extracts of tea (*C. sinensis*) that contain polyphenols such as catechins that are efficient radical scavengers as demonstrated by high ORAC scores. The efficacy of tea extracts was found to correlate with the level of tea compounds and with the levels of catechins and procyanidins, highlighting the importance of understanding botanical extract phytochemistry when assessing antioxidant performance. The highest-efficacy tea extracts were shown to prevent UV damage to hair proteins as measured by a reduction in the formation of a protein biomarker ( $m/z$  1,278).

## ACKNOWLEDGEMENTS

The authors thank The Procter & Gamble Company for funding support of this work.

## REFERENCES

- (1) T. Evans and R. R. Wickett, Eds., *Practical Modern Hair Science* (Allured Publishing Corporation, Carol Stream, IL, 2012).
- (2) C. M. Pande and J. Jachowicz, Hair photodamage: measurement and prevention, *J. Soc. Cosmet. Chem.*, **44**, 109–122 (1993).
- (3) E. Hoting and M. Zimmerman, Photochemical alteration in human hair. Part III: investigation of internal lipids, *J. Soc. Cosmet. Chem.*, **47**(4), 201–211 (1996).
- (4) W. Korytowski, B. Pilas, T. Sarna, and B. Kalyanaraman, Photoinduced generation of hydrogen peroxide and hydroxyl radicals in melanins, *Photochem. Photobiol.*, **45**(2), 185–190 (1987).
- (5) J. M. Dyer, S. D. Bringans, and W. G. Bryson, Determination of photo-oxidation products within photoyellowed bleached wool proteins, *Photochem. Photobiol.*, **82**(2), 551–557 (2006).
- (6) L. J. Kirschenbaum, X. Qu, and E. T. Borish, Oxygen radicals from photoirradiated human hair: an ESR and fluorescence study, *J. Cosmet. Sci.*, **51**(3), 169–182 (2000).
- (7) K. R. Millington and L. J. Kirschenbaum, Detection of hydroxyl radicals in photoirradiated wool, cotton, nylon and polyester fabrics using a fluorescent probe, *Color. Technol.*, **118**(1), 6–14 (2002).

- (8) J. M. Marsh, R. Iveson, M. J. Flagler, M. G. Davis, A. B. Newland, K. D. Greis, Y. Sun, T. Chaudhary, and E. R. Aistrup, Role of copper in photochemical damage to hair, *Int. J. Cosmet. Sci.*, **36**(1), 32–38 (2014).
- (9) C. Cabrera, R. Giménez, and M. C. López, Determination of tea components with antioxidant activity, *J. Agric. Food Chem.*, **51**(15), 4427–4435 (2003).
- (10) W. Koch, J. Zagórska, Z. Marzec, and W. Kukula-Koch, Applications of tea (*Camellia sinensis*) and its active constituents in cosmetics, *Molecules*, **24**(23), 4277 (2019).
- (11) A. Kaur, P. Thatai, S. Sharma, and B. Sapra, Green tea extract in microemulsion: Stability, dermal sensitization and efficacy against UV induced damages, *Int. J. Pharm. Pharm. Sci.*, **8**(Suppl 1), 1–8 (2016).
- (12) M. A. Alboreadi, M. M. Al-Najdawi, Q. B. Jarrar, and S. Moshawih, Evaluation of hair growth properties of topical kombucha tea extracts, *Adv. Tradit. Med.* **22**, 151–161 (2022).
- (13) C. Nualsri, N. Lourith, and M. Kanlayavattanakul, Development and clinical evaluation of green tea hair tonic for greasy scalp treatment, *J. Cosmet. Sci.*, **67**(3), 161–166 (2016).
- (14) J. Huang, C. L. Hastings, G. P. Duffy, H. M. Kelly, J. Raeburn, D. J. Adams, and A. Heise, Supramolecular hydrogels with reverse thermal gelation properties from (oligo)tyrosine containing block copolymers, *Biomacromolecules*, **14**, 200–206 (2013).
- (15) F. W. Ward, The absorption spectra of some amino acids, *Biochem. J.*, **17**, 898–902 (1923).
- (16) M. A. Rogers, L. Langbein, S. Praetzel-Wunder, H. Winter, and J. Schweizer, Human hair keratin-associated proteins (KAPs), *Int. Rev. Cytol.*, **251**, 209–263 (2006).
- (17) C. R. Robbins and C. H. Kelly, Amino acid composition of human hair, *Text. Res. J.*, **40**, 891–896 (1970).
- (18) D. Creed, The photophysics and photochemistry of the near-UV absorbing amino acids–1. Tryptophan and its simple derivatives, *Photochem. Photobiol.*, **39**(4), 537–562 (1984).
- (19) B. Kierdaszuk, I. Gryczynski, A. Modrak-Wojcik, A. Bzowska, D. Shugar, and J. R. Lakowicz, Fluorescence of tyrosine and tryptophan in proteins using one- and two-photon excitation, *Photochem. Photobiol.*, **61**(4), 319–324 (1995).
- (20) R. V. Benasson, E. J. Land, and T. G. Truscott, *Excited States and Free Radicals in Biology and Medicine* (Oxford University Press, Oxford, United Kingdom, 1993).
- (21) J. W. Longworth, “Luminescence of Polypeptides and Proteins,” in *Excited States of Proteins and Nucleic Acids*, R. F. Steiner and I. Weinryb, Eds. (Plenum Press, New York, 1971), pp. 319–484.
- (22) C. Giulivi, N. J. Traaseth, and K. J. A. Davies, Tyrosine oxidation products: analysis and biological relevance, *Amino Acids*, **25**(3–4), 227–232 (2003).
- (23) P. Groves, J. M. Marsh, Y. Sun, T. Chaudhary, and V. Chechik, Effect of humidity on photoinduced radicals in human hair, *Free Radicals Med. Biol.*, **121**, 20–25 (2018).
- (24) P. Groves, J. Huang, A. Heise, J. Marsh, and V. Chechik, Molecular environment and reactivity in gels and colloidal solutions under identical condition, *Phys. Chem. Chem. Phys.*, **22**(21), 12267–12272 (2020).
- (25) D. I. Pattison, A. S. Rahmanto, and M. J. Davies, Photo-oxidation of proteins, *Photochem. Photobiol. Sci.*, **11**(1), 38–53 (2012).
- (26) W. A. Yehye, N. A. Rahman, A. Ariffin, S. B. A. Hamid, A. A. Alhadi, F. A. Kadir, and M. Yaeghoobi, Understanding the chemistry behind the antioxidant activities of butylated hydroxytoluene (BHT): a review, *Eur. J. Med. Chem.*, **101**, 295–312 (2015).
- (27) J. M. Marsh, M. G. Davis, M. J. Flagler, Y. Sun, T. Chaudhary, M. Mamak, D. W. McComb, R. E. A. Williams, K. D. Greis, L. Rubio, and L. Coderch, Advanced hair damage model from ultra-violet radiation in the presence of copper. *Int. J. Cosmet. Sci.*, **37**(5), 532–541 (2015).
- (28) K. R. Millington, Photoyellowing of wool. Part 2: Photoyellowing mechanisms and methods of prevention, *Color. Technol.*, **122**(6), 301–316 (2006).
- (29) E. Fernández, B. Martínez-Teipel, R. Armengol, C. Barba, and L. Coderch, Efficacy of antioxidants in human hair, *J. Photochem. Photobiol. B*, **117**, 146–156 (2012).

- (30) I. Sopyan, R. D. Permata, D. Gozali, and I. S. K. Syah, Formulation of lotion from black tea extract (*Camellia sinensis* Linnaeus) as sunscreen, *Int. J. Appl. Pharm.*, 11(1), 205–209 (2019).
- (31) S. L. Davis, J. M. Marsh, C. P. Kelly, L. Li, C. S. Tansky, R. Fang, and M. S. J. Simmonds, Protection of hair from damage induced by ultraviolet irradiation using tea (*Camellia sinensis*) extracts [published online ahead of print 20 Aug 2021], *J. Cosmet. Dermatol.*, doi: 10.1111/jocd.14387.
- (32) K. Kizawa, H. Troxler, P. Kleinert, T. Inoue, M. Toyoda, M. Morohashi, C. W. Heizmann, Characterization of the cysteine-rich calcium-binding S100A3 protein from human hair cuticles, *Biochem. Biophys. Res. Commun.*, 299(5), 857–862 (2002).